

Universality of non-normality in real complex networks

Malbor Asllani^{1,2}, Timoteo Carletti²

¹*Mathematical Institute, University of Oxford, Oxford, England, UK and*

²*Department of Mathematics and naXys, Namur Institute for Complex Systems, University of Namur, rempart de la Vierge 8, B 5000 Namur, Belgium*

Based on a detailed study involving a large set of empirical networks arising from a wide spectrum of research fields, we claim that strong non-normality is indeed a universal property in network science. Dynamical processes evolving on non-normal networks exhibit a peculiar behaviour, initial small disturbances can undergo a transient phase and be strongly amplified although the system is linearly stable. We hence propose several models to generate complex non-normal networks to explain the origin of such property. Because of the non-normality of the networked support, the comprehension of the dynamical properties goes beyond the classical linear spectral methods, while we show that the pseudo-spectrum is able to capture such behaviour. This response is very general and it challenges our understanding of natural processes grounded on real networks, as we illustrate in the Generalised Lotka-Volterra model.

Network theory [1–3] has been a groundbreaking research field in science for the last 20 years, conceivably the only one that could glue together disparate and even contrasting disciplines such as physics [1], economy [4], biology [5] or sociology [6]. A network materialises the complex interactions between the composing entities of large systems, it thus defines the natural and structural backbone for describing complex systems, which dynamics is unavoidably bound to the network properties. So far, the behaviour of networked systems has been merely studied relying on the network spectral properties, that often have been sufficient to provide qualitative answers based on local linear analysis [7–10]. However, there are relevant and generic cases [11–13] where this statement does no longer hold true. To illustrate such phenomenon, we will refer to the case of the novel concept of non-normal networks [13], namely networks with a non-normal adjacency matrix. Linear (or linearised) stable systems, evolving on top of such networks, once perturbed, exhibit a strong amplification before returning to the initial state. This transient behaviour cannot be explained by the picture provided by their spectra [14] and can have a strong impact once nonlinearities are at play. To be able to capture this dynamical response we thus employ the pseudo-spectrum [14]. This observation being already prominent *per se* from a theoretical point of view, acquires even more relevance once we realise that non-normality is widespread in real complex networks as we show in Table I (see the Supplementary Material (SM) for a more complete version). There we report a detailed study of a large dataset of networks taken from different domains, supporting thus the claim the strong non-normality is a universal property of empirical complex networks. To anticipate our findings, this mechanism definitively challenges our comprehension of the impact of the real networks' structure on natural processes. For instance, this new perspective may shed light to explain the diversity of species in ecosystems [15], the origin of cascade failures in power grids [16] or the spread of epidemics in mobility networks, just to mention few possible

applications.

Non-normal networks

Non-normality was brought to the fore for the first time to unravel natural phenomena in the context of hydrodynamics [17]. Later, with the seminal paper by Neubert & Caswell [12] it has been applied to the study of discrete structures. Here the authors proved that non-normal ecosystems manifest a high fragility to external perturbations with particular attention to food-webs architecture. However, for a long time, the non-normality property remained isolated to these communities, hence undiscovered from almost all the remaining scientific groups eventually preventing scholars to exploit its huge potential, with few notable exceptions in neuronal dynamics [18, 19]. This absence contrasts with our first main result, strong non-normality is “the rule” for the majority of directed networks found in empirical situations (see Table I and SM). Despite the few available studies, to the best of our knowledge, there is still a lack in the scientific community of a quantification of the extent at which such networks are widespread in Nature; the goal of this work is to fill this gap. Before we go further on with our discussion, let us briefly illustrate, with a prototypical example, the influence of the non-normality on the dynamics of the linear (linearised) regime of a system defined on top of a non-normal network. Let consider the system $\dot{\mathbf{x}} = \mathbf{A}\mathbf{x}$, where \mathbf{A} is a stable asymmetric matrix, namely its *spectral abscissa* is negative, $\alpha(\mathbf{A}) < 0$, where $\alpha(\mathbf{A}) := \sup \Re(\sigma(\mathbf{A}))$ and $\sigma(\mathbf{A})$ denotes the spectrum of the matrix \mathbf{A} . If \mathbf{A} is non-normal [14], it can then happen that the *numerical abscissa*, namely $\omega(\mathbf{A}) := \sup \sigma(H(\mathbf{A}))$ is positive, $\omega(\mathbf{A}) > 0$, being $H(\mathbf{A}) = (\mathbf{A} + \mathbf{A}^*)/2$ the Hermitian part of \mathbf{A} . When this condition is satisfied the system undergoes a transient growth before converging to zero, as measured by the norm of the state vector \mathbf{x} (see panel (a) Fig. 1). In case nonlinear terms were present such transient phase could bring the system far away from the equilibrium, and thus non-normality can definitively re-

Network name	nodes	links	$\omega(\mathbf{M})$	$\omega(\mathbf{M}) - \alpha(\mathbf{M})$	$\alpha_\epsilon(\mathbf{M})$	$\hat{d}_F(\mathbf{M})$	$\Delta(\mathbf{M})$
Foodwebs							
Cypress wetlands South Florida (wet season)	128	2016	296.71	132.11	167.46	1.00	0.83
Cypress wetlands South Florida (dry season)	128	2137	217.60	152.50	82.20	1.00	0.89
Little Rock Lake (Wisconsin, US)	183	2494	21.69	14.69	10.02	0.93	0.95
Biological							
Transcriptional regulation network (<i>Escherichia coli</i>)	423	578	5.11	4.11	2.52	0.93	0.81
Metabolic network (<i>Caenorhabditis Elegans</i>)	453	4596	13.44	12.44	6.89	1.00	0.98
Pairwise proteins interaction <i>Homo sapiens</i> (large)	2239	6452	15.79	13.02	4.01	0.99	0.99
Transport							
US airport 2010	1574	28236	$1.19 \cdot 10^7$	79.30	$1.19 \cdot 10^7$	1.00	0.01
Directed road transportation network 1999 (Rome, Italy)	3353	8870	$2.40 \cdot 10^4$	120.05	$2.39 \cdot 10^4$	0.28	0.08
Directed road transportation network (Chicago region, USA)	12982	39018	4.23	$4.29 \cdot 10^{-4}$	4.54	0.19	0.04
Communication							
e-mails network Democratic National Committee (2016)	2029	39264	28.00	2.00	26.37	0.89	0.53
Enron email network (1999-2003)	87273	1148072	85.14	14.54	71.05	0.99(*)	0.30
e-mails network European institution	265214	420045	76.02	6.09	70.30	0.84(*)	0.30
Citation							
Citations to Milgram's 1967 Psychology Today paper (2002)	395	1988	10.48	10.48	4.49	1.00	1.00
Articles from or citing Scientometrics, 1978-2000 (2002)	3084	10416	10.32	8.32	5.28	1.00	0.98
Citation network DBLP	12591	49743	21.50	16.82	8.45	1.00	0.87
Social							
Hyperlinks network of 2004 US election blogs	1224	19025	45.37	10.95	34.95	0.98	0.72
Reply network of the social news website Digg	30398	87627	15.92	6.56	10.18	0.97	0.61
Trust network from the online social network Epinions	75879	508837	123.00	16.47	106.96	0.80(*)	0.13

TABLE I. We report some figures for a large set of well studied real networks, which number of nodes and links span several orders of magnitude. A more complete table is available in the SM. They all result to be (weighted) non-normal networks, namely their adjacency matrix \mathbf{M} satisfies $\mathbf{M}\mathbf{M}^* \neq \mathbf{M}^*\mathbf{M}$, they possess a positive numerical abscissa (ω) - i.e. they are reactive - which is much larger than the corresponding spectral abscissa (α). Moreover the ϵ -pseudo-spectral abscissa, α_ϵ (see Methods), is positive for the value $\epsilon = 10^{-1/2}$. The normalised Henrici's departure from normality, \hat{d}_F (see Methods), is also often very large; let us observe that in few cases of very large networks, denoted with a (*), we have been able to only provide an upper bound for the latter index, by computing the 1000 largest eigenvalues. In the last column we report the measure of non-normality Δ (hereby defined) and we can appreciate its good correlation with \hat{d}_F (see also Fig. 2 panel (c)). These figures are complemented with the Figs. 1SM and 2SM where we present the pseudo-spectra for some real networks.

shape the dynamical behaviour of nonlinear systems [13]. In fact, although a system can initially be close to a stable equilibrium, due to the strong non-normality of the interacting structure of its components, it can leave this state even when a moderate external perturbation occurs [20]. This is even more striking once we abandon the deterministic approach; in fact, exogenous or demographic perturbations, always present in the surrounding environment [21], can continuously kick the system and, assisted by the non-normality, push it out of equilibrium. Since such behaviour can be captured neither by the spectrum of the linearised model, nor accurately described by the numerical abscissa, another methodological approach has to be used for estimating the influence of non-normality on the global dynamics, namely the *pseudo-spectrum* [14] (see also Methods). The latter being defined for all $\epsilon > 0$ as $\sigma_\epsilon(\mathbf{A}) := \sigma(\mathbf{A} + \mathbf{E})$, for any perturbation $\|\mathbf{E}\| \leq \epsilon$.

As already anticipated, non-normal interaction networks are common in real scenarios, spreading from biology to sociology, from communication to transport and many more (see Table I and SM). The distinguishing key for such property can be found mainly in three topological network features: first, the directionality of the links, second, their weights and last, their global hierarchical

organisation. Most of the models originally proposed for networks generation [22–24] do not take into account the directionality or the strength of interactions and focus only on the way nodes are linked to each other. Our second main result consists thus in proposing some generation models of non-normal networks (see Fig. 2 and Methods), i.e. networks whose adjacency matrix is a non-normal one, and study their pseudo-spectral properties (see Fig. 3 and Methods). Because of their abundance in real applications or in benchmark problems, we decided to work with three of the most representative networks models adapted to the non-normal framework: Erdős-Rényi (ER) [22], Watts-Strogatz (WS) [23] and Barabási-Albert (BA) [24]. The latter model results to be the most interesting one, being the difference between spectrum and pseudo-spectrum striking comparing to the two previous cases (see Methods for a discussion about other models). To understand this behaviour, let us introduce a generation model for the non-normal Scale Free network (nSF) (see panels (b) and (c) of Fig. 1). To start with, we assume, as in the seminal Barabási-Albert model, the existence of a preferential attachment process: nodes with higher degrees become more and more connected as the growth process goes on [24]. However, differently from

the latter model, we assume directed links pointing from the entering nodes to the existing node, thus in line with the Price's model [25] conceived to reproduce directed complex networks with power-law in-degree distribution. Notice that, what it actually matters here is the hierarchical organisation of nodes, as defined by [26], induced by the preferential attachment and not the broad degree distribution. Let us stress that directionality is not sufficient to have a non-normal network, indeed non-normality implies asymmetry, but the opposite is not always true. A k -regular directed ring whose adjacency matrix is thus circulant results to be normal due to its rotational symmetry [13]. The emergence of non-normality in empirical networks can thus be explained based on two factors that will be incorporated into our generating models. The first one follows a symmetry breaking process [27]: once a link between two given nodes i and j breaks the balance of the mutual interaction (namely i influences j differently from how j does on i) then the non-normality may emerge. The greater the imbalance of interaction between the nodes, the larger the possibility that the underlying network would be non-normal. To mimic this fact, we thus endowed our model of network generation with the possibility for the existing node i to make a link pointing toward the incoming node j with a smaller weight $0 \leq w_{ji} \ll w_{ij}$ or a smaller attachment probability $0 \leq p_{i \rightarrow j} \ll p_{j \rightarrow i}$ for $j > i$. The second factor is the hierarchical organisation of the directed and/or weighted links in order to maximise the non-normality (as will see in details in the next section). This is the reason why the non-normal ER and WS models, that possess low hierarchy, manifest also low non-normality at the opposite with the highly hierarchical nSF model (Fig. 3). Let us observe that the Price's model, based on the *rich gets richer* paradigm [28], allows to describe the scale-free behaviour of the distribution of citations of scientific papers, the latter being by definition a directed acyclic graph (DAG) which is the paradigmatic example of a non-normal network. Here the symmetry breaking attains its maximum level, if $w_{ij} > 0$ then $w_{ji} = 0$. Similarly, foodwebs, communication or transport networks have a high degree of non-normality because they are (almost) DAGs (see Fig. 2 panel (c)). This claim receives further support because of the observation that most of them belong to the Scale Free [1–3] and hierarchical [26, 29, 30] families of networks.

Structure of non-normal networks

To better explain the relationship between the network structure and non-normal behavior, we resort again to the concept of DAG (see Fig. 2). Because of its tree-like structure, the adjacency matrix of a DAG assumes, after a possible relabelling of the nodes (see Methods), an upper triangular form, possessing thus the strongest degree of asymmetry and in turn a high level of non-normality. Digging into this idea, we hence determine the largest DAG one can embed in the network under scrutiny, namely we try to cast the adjacency ma-

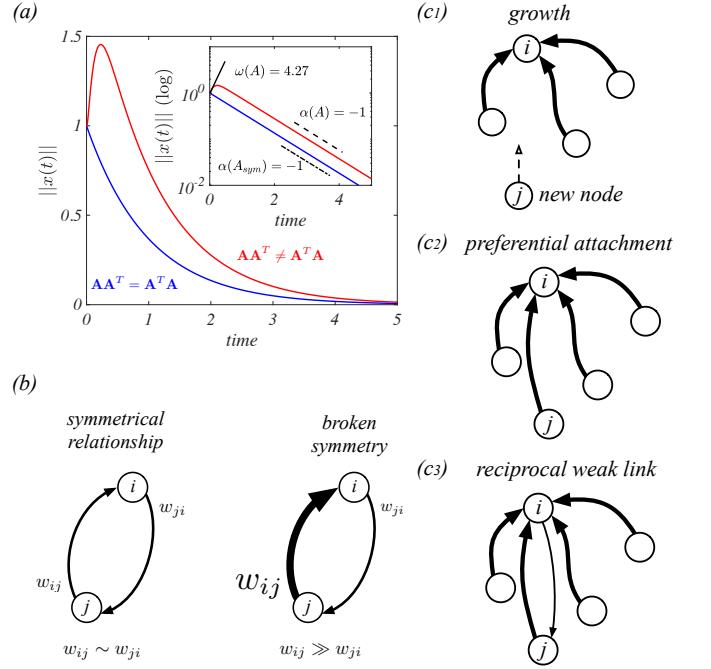


FIG. 1. Non-normal Scale Free network. (a) *non-normal transient linear dynamics*: we report the time evolution of the norm of the solution of the linear system $\dot{\mathbf{x}} = \mathbf{A}\mathbf{x}$, such that $\mathbf{A} = a\mathbf{I} + D\mathbf{L}$, $a = -1$, $D = 10$, \mathbf{I} is the identity matrix and \mathbf{L} is the Laplacian matrix of the underlying non-normal network [3]. Observe that in this way the system is stable, if a is sufficiently negative, even if $\alpha(\mathbf{M}) > 0$. The red curve corresponds to a non-normal Scale Free network (nSF), while the blue curve corresponds to the symmetric version of the same network. The inset shows the same dynamics in logarithmic scale to emphasise the long term behaviour dictated by $\alpha(\mathbf{A})$ (for both networks) and the short one, determined by $\omega(\mathbf{A})$ (for the non-normal network). (b) *local mechanism of symmetry breaking*: if j 's influence over i is larger than the reciprocal one, then the symmetry relationship is broken. (c) *generating model of nSF network*: once a new node enters in the system (c₁) it establishes, with higher probability, a link pointing toward the node with larger in-degree, i , (c₂), however with a lower probability the latter, i.e. the hub, can create a weaker link pointing in the reciprocal direction (c₃).

trix in an upper triangular form, after relabelling nodes and ordering them for increasing in-degree. Generally, this goal cannot be exactly achieved and the adjacency matrix will still contain some entries in the lower diagonal part. A simple and direct measure of non-normality will thus be the unbalance between the number of entries in the upper and lower triangular part of the adjacency matrix \mathbf{A} whose nodes have been relabelled, $\Delta := \left| \left(\sum_{i < j} \tilde{A}_{ij} - \sum_{j < i} \tilde{A}_{ij} \right) \right| / K$, where $K = \sum_{i < j} \tilde{A}_{ij} + \sum_{j < i} \tilde{A}_{ij}$. This measure can be grounded on solid physical bases. Indeed, one can consider a diffusion process supported by such network; the subgraph determined by the upper triangular part of the adjacency matrix tends to accumulate the mass spreading on the

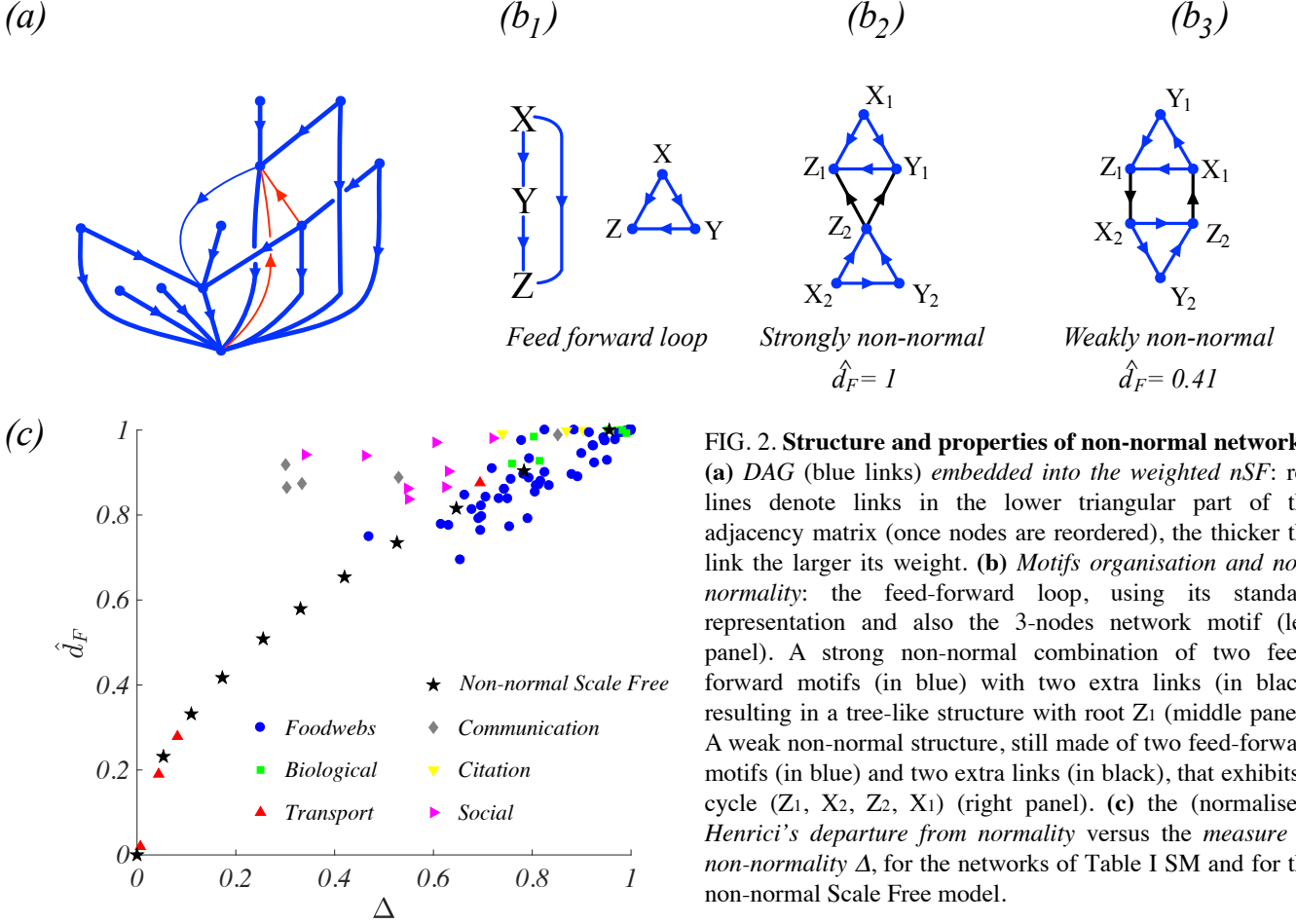


FIG. 2. Structure and properties of non-normal networks. (a) DAG (blue links) embedded into the weighted *nSF*: red lines denote links in the lower triangular part of the adjacency matrix (once nodes are reordered), the thicker the link the larger its weight. (b) Motifs organisation and non-normality: the feed-forward loop, using its standard representation and also the 3-nodes network motif (left panel). A strong non-normal combination of two feed-forward motifs (in blue) with two extra links (in black) resulting in a tree-like structure with root Z_1 (middle panel). A weak non-normal structure, still made of two feed-forward motifs (in blue) and two extra links (in black), that exhibits a cycle (Z_1, X_2, Z_2, X_1) (right panel). (c) the (normalised) Henrici's departure from normality versus the measure of non-normality Δ , for the networks of Table I SM and for the non-normal Scale Free model.

network into its terminal nodes. On the other hand, the lower triangular part attempts to reverse such process and removes mass from these nodes. This is exactly the meaning of Δ . Observe that the measure we here introduce evaluates the asymmetry of the adjacency matrix, but as mentioned earlier this not necessary always implies the non-normality. For instance in the case of a circulant adjacency matrix no accumulation will ever take place. However, such structures are unlikely to occur in networks with high hierarchy. In panel (a) of Fig. 2 we show a small non-normal Scale Free network where we highlighted the “best” arrangement of the directed edges, i.e. the largest embedded DAG, obtained applying the above described procedure (see Methods). Let us observe that non-normality can be directly measured using the Henrici's departure from normality (see Methods and [14]), a tool from matrix analysis based on the Frobenius norm and the eigenvalues of the adjacency matrix, the larger the index the stronger the non-normality. In panel (c) of Fig. 2 we show that the normalised Henrici index strongly correlates with the above introduced measure Δ for almost all the real networks studied in this work and for the non-normal Scale Free model (see also Methods for a similar result involving the synthetic networks built using the other proposed generation models).

Many networked systems, e.g. in biology, in social sciences or in communication, can be decomposed into a large number of basic small motifs, and the dynamical properties of the system strongly depend on the latter [26, 31, 32]. Non-normality is grounded on a similar observation but now the network motifs should be oriented/organised in such a way to construct a macrostructure that resembles as much as possible to a DAG. To support this claim, we present a stereotyped example the *feed-forward loop* (see panel (b) Fig. 2), being such motifs at the roots of several relevant applications [31]. We thus take two copies of such 3×3 directed motif and we allowed 2 directed extra links to be used to connect the two motifs. This setting determines several configurations and for each one, we compute the normalised Henrici's departure from normality. We report generic results in panel (b) of Fig. 2 showing that the coupling obtained in panel (b2) is strongly non-normal, $\hat{d}_F = 1$ and the embedded DAG coincides with the network itself; from a diffusion process point of view, one can realise by direct inspection that the links directionality “pushes” the mass to accumulate on the node Z_1 . On the other hand the structure presented in panel (b3) is weakly non-normal, $\hat{d}_F = 0.41$ and the embedded DAG doesn't contain the link $Z_2 \rightarrow X_1$. From a dynamical perspective,

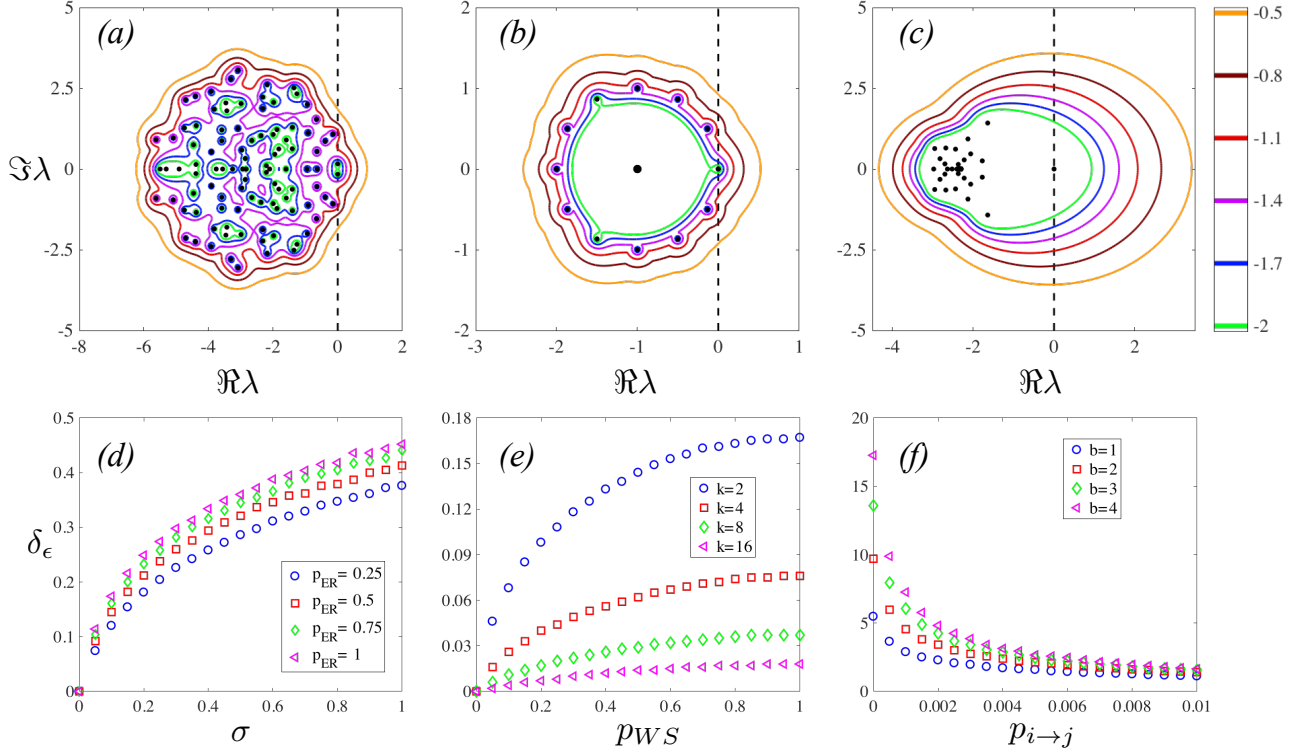


FIG. 3. **Generation models of non-normal networks.** (Upper panels) spectra and pseudo-spectra of non-normal models: (a) Erdős-Rényi (ER) with links probability $p_{ER} = 0.1$ and weights from a normal distribution $\mathcal{N}(0, 1)$, (b) (unweighted) Watts-Strogatz (WS) with initial number of neighbour nodes $k = 2$ and rewiring probability $p_{WS} = 1$, (c) non-normal scale free network (nSF) with probability of backward links $p_{i \rightarrow j} = 0.001$ for $j > i$ and weights from a uniform distribution, $\mathcal{U}[0, 1]$. The colour bar on the right, represents the different levels of $\|\mathbf{E}\|$. (Lower panels) the difference between ϵ -pseudoabscissa of the original network and its Hermitian part, $\delta_\epsilon = \alpha_\epsilon(\mathbf{A}) - \alpha_\epsilon(H(\mathbf{A}))$, as expected this quantity is always positive, being the pseudo-spectrum larger for a non-normal matrix than for a normal one [14], for any given fixed $\epsilon > 0$, (d) ER with weights from a normal distribution $\mathcal{N}(0, \sigma)$ for several values of the variance and different links probabilities, p_{ER} , (e) (unweighted) WS for different rewiring probabilities p_{WS} and different initial number of neighbour nodes k , (f) nSF with varying backward links probability $p_{i \rightarrow j}$ and different upper bound, b , of the uniform distribution from which the weights are chosen, $\mathcal{U}[0, b]$. In all the cases the networks are made by 100 nodes and the adjacency matrices have been diagonally shifted with their respective spectral abscissa $\alpha(\mathbf{A})$ to set the real part of the maximum of each spectrum exactly at 0. The pseudo-spectra have been numerically computed using the software *Eigtool* [34].

the added links create a cycle (Z_1, X_2, Z_2, X_1) that attracts the total mass, preventing thus the accumulation on a node. The bridge we cast between network motifs, their hierarchical organisation and non-normality could open the way to a new comprehension of the global behaviour of networked dynamical systems and to *ad hoc* models of networks generation.

Dynamics on non-normal networks

Stability is one of the most important properties that portrays the mechanism responsible for the emergence of collective phenomena [10]. May [7, 8] intuited the importance of the interactions structure already in the early 70's when he studied the stability of large interacting populations divided into communities in the context of ecology. Choosing the interaction strengths from a normal distribution $\mathcal{N}(0, \sigma)$, he proved that once the ecosystem becomes large enough it loses its stability, as consequence of the circular law [33]. Consequently, an

increase of the numbers of the interconnected components will transit the system to instability. To further understand the interplay of non-normal topology and dynamics, we analyse for illustration purpose the master stability function [10] for the Generalised Lotka-Volterra model, a paradigmatic framework to understand competition and mutualism among interacting species [7–9]. It has been recently shown that such models become more vulnerable, and thus the systems less stable, when the competitiveness among species decreases [9]. This is clearly visible in Fig. 4 where the spectra shift from the left to the right of the imaginary axis once the mutualism increases. Although the system remains clearly stable for a strong competitive setting (panels (a) and (b)), we can observe that the ϵ -pseudo spectral abscissa [14], $\alpha_\epsilon(\mathbf{A}) := \sup \Re \sigma_\epsilon(\mathbf{A})$, is positive and larger for structured systems than for random ones [8]. This implies that the system can be easily destabilised by (relatively) small fluctuations due to demographic, thermal or endogenous

noise, always present in the surrounding environment and that are amplified due to the non-normality (see Methods). This remark can have important consequences in the understanding of the problem of coexistence of multiple species in a harsh competitive environment, e.g. in the case of the paradox of the plankton [35] for which field observations are at odds with the Principle of Competitive Exclusion [8].

Discussion and conclusions

The impact of links directionality has been studied in the framework of patterns formation [20] but still relying on the spectral property of the directed network. In the present work we go further by considering non-normal networks possessing intriguing dynamical behaviours, that cannot be captured by the spectral analysis. Recently [13], it has been shown that when the individuals of a single inhibitor species affected by the Allee effect [36] - i.e. the impossibility to survive for small initial densities - are allowed to diffuse on a non-normal network, then they may reverse their fate and survive even if in low number. This particular attitude can be further generalised to explain the spreading of epidemics (e.g. measles [13]) among human beings moving using transportation networks [37]. This example can be cast

in the more general framework of patterns formation and improves the classical Turing instability scenario which requires at least two (activator-inhibitor) species to determine the pattern onset [38]. Indeed, the non-normal network played the decisive role of forcing the species to self-activate in contrast with its true nature. This result may open new research scenarios such for instance, the zygotic cells differentiation in the initial phase of embryo development [39] where it has been observed that the identical cells are organised in a network arrangement before starting the morphogenesis. To conclude, our findings are manifold; first we provided strong support to the claim concerning the universality of non-normal networks in many real scenarios; second we proposed generation models of non-normal networks, we studied their pseudo-spectral properties and the peculiar features exhibited by systems once defined on top of the latter networks with respect to the symmetrised counterparts. Finally, we provided measures of network non-normality based on their structure. These results state that stability analysis of real networked systems should be equipped with adequate instruments, such as the pseudo-spectrum, to fully understand complex behaviours. The same principles are not limited to the examples brought here, but they naturally extend to general networked dynamical systems.

-
- [1] R. Albert and A.-L. Barabási, *Rev. Mod. Phys.* **74**, 47 (2002)
 - [2] S. Boccaletti, V. Latora, Y. Moreno, M. Chavez and D.-U. Hwang, *Phys. Rep.* **424**, 175–308 (2006)
 - [3] M. E. J. Newman, *Networks: An Introduction*, Oxford University Press (2010)
 - [4] M. O. Jackson, *Social and economic networks*, Princeton University Press (2008)
 - [5] A.-L. Barabási, N. Gulbahce and J. Loscalzo, *Nat. Rev. Genet.* **12**, 56–68 (2011)
 - [6] S. Wasserman and K. Faust, *Social Network Analysis: Methods and Applications*, Cambridge University Press (1994)
 - [7] R. M. May, *Nature* **238**, 413–414 (1972)
 - [8] S. Allesina and S. Tang, *Nature* **483**, 205–208 (2012)
 - [9] K. Z. Coyte, J. Schuleter and K. R. Foster, *Science* **350**, 663–666 (2015)
 - [10] L. M. Pecora and T. L. Carroll, *Phys. Rev. Lett.* **80**, 2109 (1998)
 - [11] B. Ravoori, A.D. Cohen, J. Sun, A.E. Motter, T.E. Murphy and R. Roy, *Phys. Rev. Lett.* **107**, 034102 (2011)
 - [12] M. G. Neubert and H. Caswell, *Ecology* **78**(3), 653–665 (1997)
 - [13] M. Asllani and T. Carletti, *Phys. Rev. E*, **97**(4) 042302 (2018)
 - [14] L. N. Trefethen and M. Embree, *Spectra and pseudospectra: The behavior of nonnormal matrices and operators*, Princeton University Press (2005)
 - [15] P. Chesson, *Annu. Rev. Ecol. Evol. Syst.* **31**, 343–366 (2000)
 - [16] S. V. Buldyrev, R. Parshani, G. Paul, H. E. Stanley and S. Havlin, *Nature* **464**, 1025–1028 (2010)
 - [17] L. N. Trefethen, A. E. Trefethen, S. C. Reddy and T. A. Driscoll, *Science* **261**, 578–584 (1993)
 - [18] B. K. Murphy and K. D. Miller, *Neuron* **4**, 635–648 (2009)
 - [19] G. Hennequin, T. P. Vogels and W. Gerstner, *Phys. Rev. E* **86**, 011909 (2012)
 - [20] M. Asllani, J. D. Challenger, F. S. Pavone, L. Sacconi and D. Fanelli, *Nat. Commun.* **5**, 4517 (2014)
 - [21] C. W. Gardiner, *Handbook of Stochastic Methods: for Physics, Chemistry and the Natural Sciences*, Springer 3ed (2004)
 - [22] P. Erdős and A. Rényi, *Publ. Math. Inst. Hung. Acad. Sci.* **5**, 17–61 (1960)
 - [23] D. J. Watts and S. H. Strogatz, *Nature* **393**, 440–442 (1998)
 - [24] A.-L. Barabási and R. Albert, *Science* **286**, 509–512 (1999)
 - [25] D. J. de Solla Price, *Science* **149**, 510–515 (1965)
 - [26] B. Corominas-Murtra, J. Goñi, R. V. Solé, and C. Rodríguez-Caso, *PNAS* **110**, 13316–13321 (2013)
 - [27] P. W. Anderson, *Science* **177**, 393–396 (1972)
 - [28] H. A. Simon, *Biometrika* **42**, 425–440 (1955)
 - [29] E. B. Ravasz and A.-L. Barabási, *Phys. Rev. E* **67**, 026112 (2003)
 - [30] D. Czégel and G. Palla, *Scie. Rep.* **5**, 17994 (2015)
 - [31] R. Milo, S. Shen-Orr, S. Itzkovitz, N. Kashtan, D. Chklovskii and U. Alon, *Science* **298**, 824–827 (2002)
 - [32] R. Milo, S. Itzkovitz, N. Kashtan, R. Levitt, S. Shen-Orr, I. Ayzenshtat, M. Sheffer and U. Alon, *Science* **303**, 1538–42 (2004)
 - [33] According to Tao & Vu, [40], the eigenvalues of a $n \times n$ matrix, whose entries are i.i.d. random variables drawn

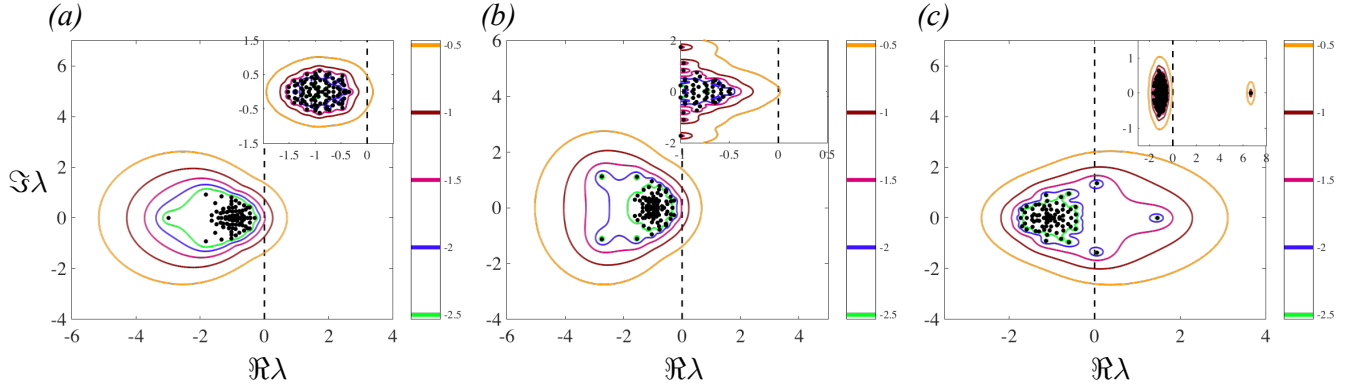


FIG. 4. **The Generalised Lotka-Volterra model:** $\dot{x}_i = x_i(r_i - s_i x_i + \sum_{j \neq i} M_{ij} x_j)$. We consider an ecosystem composed by 100 species; for a sake of simplicity, the intra-species interactions are set equal, $s_i = 1 \forall i$, and \mathbf{M} is the (weighted and signed) adjacency matrix of a nSF scale free non-normal network for the structured case (main panels) or a random matrix (insets) which weights are drawn from a normal distribution $\mathcal{N}(0, 1/\sqrt{n})$. In the structured cases the strengths in the upper triangular part of the matrix \mathbf{M} are 4 times larger than in the lower one, enhancing thus the non-normality as one can appreciate from the pseudo-spectrum levels. The Master stability function close to a stable equilibrium point is analysed using the pseudo-spectra for several cases according to the signs of the interaction strengths: (a) competition $(-/-)$, (b) prey-predator $(-/+)$ and (c) mutualism $(+/+)$. We can observe that even if the system is stable (panels (a) and (b)), the ϵ -pseudo abscissa is positive for large enough ϵ , inducing thus an unstable system behaviour if the perturbation (in the adjacency matrix and/or in the initial conditions) is strong enough; moreover this effect is more pronounced in the structured systems than in the random ones being the ϵ -levels much larger for the former model for the same value of ϵ . The pseudo-spectra have been numerically computed using the software *Eigtool* [34].

from a distribution with 0 mean and variance 1, lie in a disc of radius \sqrt{n} with probability 1 for large enough n .

- [34] Eigtool software <http://www.cs.ox.ac.uk/projects/pseudospectra/eigtool/>
- [35] G. E. Hutchinson, *Am. Nat.* **95**, 137–145 (1961)
- [36] W. C. Allee and E. Bowen, *J. Exp. Zool.* **61**(2), 185–207 (1932)
- [37] V. Colizza, A. Barrat, M. Barthélemy and A. Vespignani, *PNAS* **103**, 2015–2020 (2006)
- [38] A. M. Turing, *Phil. Trans. R. Soc. B* **237**, 37–72 (1952)
- [39] R. Schnabel, M. Bischoff, A. Hintze, A.-K. Schulz, A. Hejnola, H. Meinhardt and H. Hutter, *Dev. Biol.* **294**, 418–431 (2006)
- [40] T. Tao and V. H. Vu, *Commun. Contemp. Math.* **10**(2), 261–307 (2008)

Acknowledgments The work of M.A. and T.C. presents research results of the Belgian Network DYSCO, funded by the Interuniversity Attraction Poles Programme, initiated by the Belgian State, Science Policy Office. The work of M.A. is also supported by a FRS-FNRS Postdoctoral Fellowship. Particular gratitude goes to D. Fanelli and R. Lambiotte for useful discussions. The authors acknowledge also P. K. Maini for reading the manuscript.

Methods

Non-normal matrices and their pseudo-spectra

A $M \times M$ real matrix \mathbf{A} is said to be *non-normal* if it is not diagonalisable by a unitary matrix, namely its eigenvectors are not orthogonal to each other; this statement is equivalent to require $\mathbf{A}\mathbf{A}^* \neq \mathbf{A}^*\mathbf{A}$, where \mathbf{A}^* denotes the conjugate and transpose matrix [41].

There exist several measures of non-normality in the literature [14, 42], we will hereby limit ourselves to present the ones suitable for our analysis and we refer the interested reader to above cited sources. We also limit ourselves to the case of continuous time dynamical systems (Ordinary Differential Equation), the reader must however be aware that an analogous theory exists for discrete time dynamical systems (maps), also exhibiting peculiar behaviours.

Non-normality measures and transient growth

Non-normal linear dynamical systems exhibit a peculiar time evolution, the transient phase being potentially very different from the case of normal ones. In population dy-

namics [12] the *reactivity* is used for evaluating the ecological resilience, the latter, referred to as the *numerical abscissa* [14], suits also our purpose. For a given $M \times M$ real matrix \mathbf{A} it is defined by:

$$\omega(\mathbf{A}) := \sup \sigma \left((\mathbf{A} + \mathbf{A}^*)/2 \right), \quad (1)$$

where $\sigma(\mathbf{A})$ denotes the spectrum of the matrix \mathbf{A} . Consider thus the linear ODE, $\frac{d\mathbf{x}}{dt} = \mathbf{A}\mathbf{x}$ and let assume \mathbf{A} to be a stable matrix [41], i.e. $\alpha(\mathbf{A}) := \sup \Re \sigma(\mathbf{A}) < 0$; if the numerical abscissa takes negative values then the orbits exponentially approach the fixed point, on the other hand if $\omega(\mathbf{A}) > 0$, then a transient growth occurs whose size is proportional to the numerical abscissa, providing thus a proxy for the magnitude of the non-normality of \mathbf{A} (see Fig. 1 in the main text and Fig. 5).

Such transient growth can be understood by analysing the time evolution of the Euclidian norm of the solution $\|\mathbf{x}\| = \sqrt{x_1^2 + x_2^2 + \dots + x_M^2}$. Indeed the *numerical abscissa* describes the short time behaviour of the solution (the limit $t \rightarrow 0^+$), in fact calculating:

$$\begin{aligned} \max_{\|\mathbf{x}_0\| \neq 0} \left[\left(\frac{1}{\|\mathbf{x}\|} \frac{d\|\mathbf{x}\|}{dt} \right) \right]_{t=0} &= \max_{\|\mathbf{x}_0\| \neq 0} \left[\left(\frac{1}{\|\mathbf{x}\|} \frac{d\sqrt{\mathbf{x}^* \mathbf{x}}}{dt} \right) \right]_{t=0} = \max_{\|\mathbf{x}_0\| \neq 0} \left[\left(\frac{\mathbf{x}^* d\mathbf{x}/dt + (d\mathbf{x}/dt)^* \mathbf{x}}{2\|\mathbf{x}\|^2} \right) \right]_{t=0} \\ &= \max_{\|\mathbf{x}_0\| \neq 0} \left[\left(\frac{\mathbf{x}^* (\mathbf{A} + \mathbf{A}^*) \mathbf{x}}{2\|\mathbf{x}\|^2} \right) \right]_{t=0} = \max_{\|\mathbf{x}_0\| \neq 0} \left[\frac{\mathbf{x}_0^* H(\mathbf{A}) \mathbf{x}_0}{\mathbf{x}_0^* \mathbf{x}_0} \right], \end{aligned} \quad (2)$$

where \mathbf{x}_0 is the initial condition for the solution \mathbf{x} . One can recognise that $H(\mathbf{A}) = (\mathbf{A} + \mathbf{A}^*)/2$ is the Hermitian part of \mathbf{A} , hence according to the Rayleigh's principle [41] the rightmost term of Eq. (2) is equal to the largest eigenvalue of $H(\mathbf{A})$. We can thus conclude that $\omega(\mathbf{A}) = \sup \sigma(H(\mathbf{A}))$ provides the initial behaviour of the norm of \mathbf{x} , if $\omega(\mathbf{A}) > 0$ then $\|\mathbf{x}(t)\|$ will necessarily increase for small positive times. Observe that if \mathbf{A} is stable and normal then it is necessarily non reactive, $\omega(\mathbf{A}) < 0$, on the other hand if \mathbf{A} is non normal, then $\omega(\mathbf{A})$ can have both signs. Notice that this measure does not depend anymore on the initial conditions, meaning that it characterises the intrinsic properties of the matrix \mathbf{A} and not of a specific solution.

The second limit we are interested in, is the long time behaviour of the solution, namely $t \rightarrow +\infty$. This can be studied using the *spectral abscissa* of the matrix \mathbf{A} , denoted by $\alpha(\mathbf{A})$ and defined by:

$$\alpha(\mathbf{A}) := \max_{\|\mathbf{x}_0\| \neq 0} \left[\lim_{t \rightarrow +\infty} \left(\frac{1}{\|\mathbf{x}\|} \frac{d\|\mathbf{x}\|}{dt} \right) \right]. \quad (3)$$

It is well known that the eigenvalue with the largest real part completely determines the asymptotic behaviour of the solution of the ODE, thus one can compute the spectral abscissa as $\alpha(\mathbf{A}) = \sup \Re(\sigma(\mathbf{A}))$.

We can hence conclude by observing that, although $\alpha(\mathbf{A}) < 0$, if $\omega(\mathbf{A}) > 0$ then the equilibrium will be stable but a transient growth will emerge in the short time regime producing a deviation from the steady exponential decay of stable normal systems. The following simple but stereotypical example well illustrates this behaviour. Let us analyse the time evolution of the norm of the solution of the linear ODE system involving the following matrices \mathbf{A}_i , $i = 1, 2$

$$\mathbf{A}_1 = \begin{pmatrix} -1 & 1 \\ 0 & -2 \end{pmatrix} \quad \text{and} \quad \mathbf{A}_2 = \begin{pmatrix} -1 & 10 \\ 0 & -2 \end{pmatrix}.$$

A straightforward computation allows to obtain the numerical abscissa, $\omega(\mathbf{A}_1) = -0.79 < 0$ and $\omega(\mathbf{A}_2) = 3.52 > 0$, and the spectral abscissa $\alpha(\mathbf{A}_1) = \alpha(\mathbf{A}_2) = -1$. Although both matrices possess the same spectral abscissa, the existence of a positive numerical abscissa for the second matrix determines a transient growth to occur (see Fig. 5).

Pseudo-spectrum: a powerful technique for measuring the non-normal dynamics

The numerical abscissa is indeed a very natural concept however it is not sufficient to completely describe the transient growth, in particular it doesn't allow to

compute the maximum amplification of the initial conditions; for this reason one has to recur to the pseudo-spectrum [14]. The latter being defined for all $\epsilon > 0$ as the spectrum of the perturbed matrix $\mathbf{A} + \mathbf{E}$, for any perturbation $\|\mathbf{E}\| \leq \epsilon$, or in an equivalent way [14] as the set of complex numbers z such that $\|(\mathbf{A} - z\mathbf{I})\mathbf{v}\| \leq \epsilon$ for some complex unitary vector \mathbf{v} . Let us notice that this second definition allows to introduce the concept of pseudo-eigenvector i.e. \mathbf{v} .

For any positive ϵ one can define the ϵ -pseudo-abcissa as the maximum of the real part of the ϵ -pseudo-spectrum and use the latter to provide useful bounds on the amplification of the initial condition. One can in fact prove [14] that for all stable matrix \mathbf{A} and $\epsilon > 0$

$$\|e^{\mathbf{A}t}\| \leq \frac{L_\epsilon}{2\pi\epsilon} e^{\alpha_\epsilon(\mathbf{A})t} \quad \forall t > 0,$$

being L_ϵ the length of the boundary of the ϵ -pseudo-spectrum. On the other hand, defining the Kreiss constant $\mathcal{K}(\mathbf{A}) = \sup_{\epsilon > 0} \alpha_\epsilon(\mathbf{A})/\epsilon$, one has the lower bound

$$\sup_{t \geq 0} \|e^{\mathbf{A}t}\| \geq \mathcal{K}(\mathbf{A}).$$

Let us conclude this subsection by observing that the pseudo-spectrum can be defined for all matrices, being a generalisation of the classical spectral methods, with however a peculiar difference; in the case of non-normal matrices the pseudo-spectrum is much “larger” than the spectrum, e.g. $\alpha_\epsilon(\mathbf{A}) - \alpha(\mathbf{A}) \gg 0$. If one thus takes a non-normal (adjacency) matrix \mathbf{A} and compares its pseudo-spectrum with the one of the Hermitian part, $H(\mathbf{A})$, then one can conclude that $\alpha_\epsilon(\mathbf{A}) - \alpha_\epsilon(H(\mathbf{A})) > 0$. This result can be observed in Fig. 3 for three non-normal networks ER, WS and SF.

Non-normality measures and spectral properties

The Frobenius norm of a normal matrix is given by $\|\mathbf{A}\|_F^2 = \text{tr}(\mathbf{A}^*\mathbf{A}) = \sum_{i=1}^M |\lambda_i|^2$ where λ_i are the eigenvalues of the matrix; one can thus define the *Henrici's departure from normality* [14] for a non-normal matrix \mathbf{A} by:

$$d_F(\mathbf{A}) = \sqrt{\|\mathbf{A}\|_F^2 - \sum_{i=1}^M |\lambda_i|^2}.$$

It attains its minimum once the matrix is indeed normal and then increases as long as the matrix deviates from normality. Let us observe that the multiplication of a matrix by a scalar increases the value of such index, hence to remove this issue one can define a normalised index:

$$\hat{d}_F(\mathbf{A}) = \frac{\sqrt{\|\mathbf{A}\|_F^2 - \sum_{i=1}^M |\lambda_i|^2}}{\|\mathbf{A}\|_F},$$

whose range is $[0, 1]$, the lower bound being achieved for a normal matrix while the upper one for a strong non-normal one. This measure will be particularly

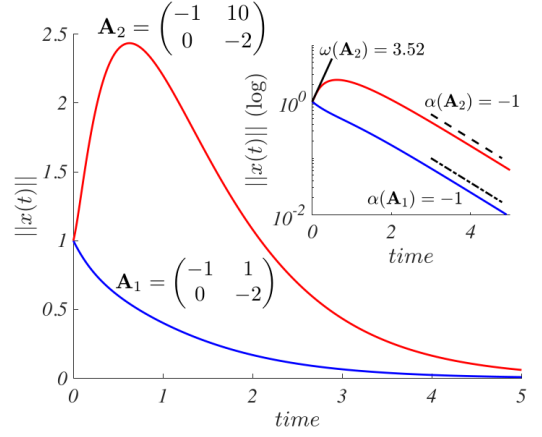


FIG. 5. **Time evolution of the norm of the solution of the linear ODE $\dot{\mathbf{x}} = \mathbf{A}\mathbf{x}$.** The red curve corresponds to a non-normal matrix $\omega(\mathbf{A}_2) = 3.52$ while the blue curve to a normal one $\omega(\mathbf{A}_1) = -0.79$, one can clearly appreciate the temporal growth arising in the former case. In the inset we still report the norm of the solution but in logarithmic scale to emphasise the short time behaviour described by the numerical abscissa (the straight black line has slope 3.52) and the long time one related to the spectral abscissa (the dashed and dot dashed straight lines have slope -1).

suitable to compare weighted networks, whose adjacency matrices are non-normal, or networks of different sizes.

Global structure of non-normal networks

The aim of this section is to discuss the global structure of non-normal network, emphasising the role of the directed acyclic graph (DAG) and the hierarchical organisation of motifs.

A simple measure of non-normality

As we already discussed in the main text a directed acyclic graph (DAG) is the paradigmatic example of a non-normal network, whose tree-like structure can result (after possibly relabel the nodes) into an adjacency matrix containing elements only in its upper triangular part [43]. For a generic matrix, one can thus define the unbalance between the number of entries in the upper and lower triangular part, or using the language of the networks

$$\Delta(\mathbf{A}) := \frac{\left| \left(\sum_{i < j} \tilde{A}_{ij} - \sum_{j < i} \tilde{A}_{ij} \right) \right|}{\left(\sum_{i < j} \tilde{A}_{ij} + \sum_{j < i} \tilde{A}_{ij} \right)}, \quad (4)$$

where \tilde{A}_{ij} are the entries of the final relabelled adjacency matrix.

While it can be relatively easy to determine a DAG, and compute Δ , once we have a drawing of a (small enough) network, this task becomes hard starting from the adjacency matrix or a large network. We observe that the simple operation of relabelling the nodes can change the value of Δ and the latter increases the larger the num-

ber of entries in the adjacency matrix are in upper triangular part, namely links $i \rightarrow j$ where $j > i$. Having in mind these observations we created an algorithm aiming at maximising Δ once couples of nodes are relabelled, i.e. rows and columns of the adjacency matrix are swapped. To overcome the combinatorial difficulty of the problem, we resorted to a Simulate Annealing method [44] to get an accurate solution in a relatively short time.

Algorithm 1. Determine the best DAG embed in \mathbf{A}_0 and maximise $\Delta(\mathbf{A}_0)$. The following parameters should be passed to the algorithm, α is the “cooling coefficient”, k_{max} the maximum allowed number of iterations and δ the precision required. The algorithm returns the reorganised adjacency matrix \mathbf{A}_1 and the maximised value for $\Delta(\mathbf{A}_1)$. The **swap** function exchanges two randomly chosen rows and columns in the matrix \mathbf{A}_0 by left/right multiplication with a permutation matrix, to obtain the new matrix \mathbf{A}_1 .

```

1: inputs:  $\mathbf{A}_0, \alpha, k_{max}, \delta$ 
2: outputs:  $\mathbf{A}_1, \Delta(\mathbf{A}_1)$ 
3: initialisation:  $T = 1, k = 0, \delta_0 = 1$ 
4:  $f_0 \leftarrow 1 - \Delta(\mathbf{A}_0)$ 
5: while ( $k \leq k_{max}$  and  $\delta_0 > \delta$ ) do
6:    $k \leftarrow k + 1$ 
7:    $\mathbf{A}_1 \leftarrow \text{swap}(\mathbf{A}_0)$ 
8:    $f_1 \leftarrow 1 - \Delta(\mathbf{A}_1)$ 
9:   if  $f_1 < f_0$  then
10:     $\delta_0 = |f_1 - f_0|$ 
11:     $\mathbf{A}_0 \leftarrow \mathbf{A}_1$ 
12:     $f_0 \leftarrow f_1$ 
13:     $T \leftarrow \alpha T$ 
14:   else
15:     $u \leftarrow e^{-(f_1 - f_0)/T}$ 
16:     $r \leftarrow \mathcal{U}[0, 1]$ 
17:    if  $r < u$  then
18:       $\mathbf{A}_0 \leftarrow \mathbf{A}_1$ 
19:       $f_0 \leftarrow f_1$ 
20:    end if
21:   end if
22: end while

```

A pseudo-code is presented in Algorithm 1 and the generic convergence behaviour of the maximisation process is shown in Fig. 6. To benchmark the latter we realised the follow tests; first we created an initial network whose adjacency matrix is \mathbf{A}_0 and $\Delta_0 = \Delta(\mathbf{A}_0)$ is computed, then we apply the maximisation algorithm 1 to determine a sequence of matrices \mathbf{A}_k with the associated $\Delta_k = \Delta(\mathbf{A}_k)$ as long as the stopping criteria of the algorithm are not met. One can appreciate the sudden growth of Δ_k after relatively few steps and the convergence to $\Delta_{fin} = \Delta(\mathbf{A}_{fin})$. The four panels of Fig. 6 show the behaviour for the non-normal Scale Free and non-normal Erdős-Rényi for some configuration of network sizes and model parameters. One can observe the very similar behaviour in all cases and the capability of the algorithm to transform a generic adjacency matrix into an almost upper triangular one (see insets).

In the main text, we have shown (see Fig. 2 panel (c)) the existence of a correlation between the values of the

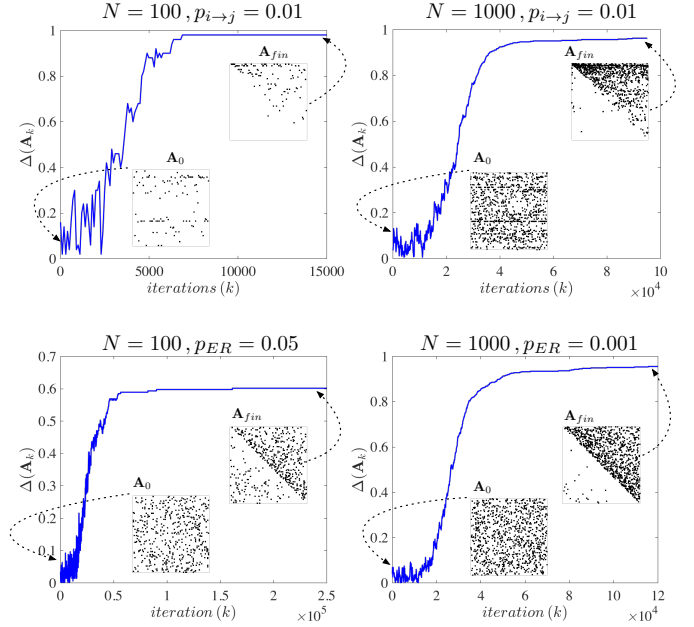


FIG. 6. Convergence of the maximisation process. We report some typical evolutions of $\Delta(\mathbf{A}_k)$ as a function of the iteration number k for a nSF network (top panels) with $p_{i \rightarrow j} = 0.01$ and $N = 100$ (left), $N = 1000$ (right), non-normal ER (bottom panels) with $(p_{ER}, N) = (0.05, 100)$ (left) and $(p_{ER}, N) = (0.001, 1000)$ (right). We can observe that the solution approaches a stationary value Δ_{ini} with a number of iterations slowly increasing with the network size. The “cooling” parameter has been fixed to $\alpha = 0.99$.

Henrici’s departure from normality and Δ computed for several real networks, this evidence is even stronger for the synthetic networks built using the generating models we hereby propose, results are reported in Fig. 7 for the nSF and the non-normal ER networks.

Network motifs and non-normality

Motifs are small subgraphs present in complex networks whose frequencies are significantly higher than those in randomised networks. Such small basic motifs, composed by 3 – 4 nodes, strongly influence the dynamical properties of the whole networked system [31, 32], arising in a very large spectrum of applications. One can thus expect a similar impact to be possible in the non-normal case as well; we hereby show that this statement holds true provided we add a constraint of the hierarchical organisation of such motifs. In other words, non-normality is a global property of the network that can be explained by the presence of motifs interconnected among them in the “right way” to avoid cycles.

For a sake of concreteness we provide results to support the evidence of our claim for the *feed-forward loop* (see panel (b) Fig. 2), because this motif arises in several relevant applications [31, 32]. We thus take two copies of such motif, fix the number of links to be

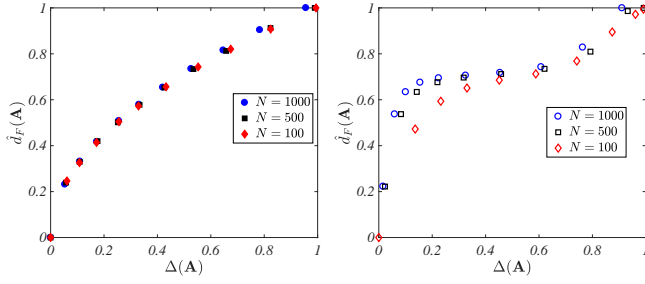


FIG. 7. **Henrici's departure from normality versus Δ .** Left panel: for several values of $p_{i \rightarrow j} \in (0, 1)$ and for several network sizes we build a non-normal Scale Free network and we computed \hat{d}_F and Δ using the optimisation algorithm 1. Right panel: for several values of $p_{ER} \in (0, 1)$ and for several network sizes we build a non-normal Erdős-Rényi network and we computed \hat{d}_F and Δ using the optimisation algorithm 1.

used to interconnect them and we create all the possible resulting networks made by 6 nodes and 8 links. For each one of such networks, we compute the Henrici's departure from normality. We report in panel (b) of Fig. 2 two results, which present nevertheless a generic behaviour. There are configurations (b2) that result to be strongly non-normal, as testified by the large values of \hat{d}_F and Δ , while for other cases (b3) the non-normality is weaker. From a linear dynamical perspective, the former cases result to behave like directed trees, i.e. having sink attracting the system mass, while the latter ones exhibits directed cycles, preventing the mass to accumulate.

Models for generation of non-normal networks

Non-normal networks have been defined [13] as networks whose adjacency matrices are non-normal ones. The aim of this section is to present and describe some new model of networks generation exhibiting the non-normality property. As stated in the main text, the key ingredients to achieve such goal are the directionality of the links, their weights and their global hierarchical organisation.

We start with probably the first known model to generate non-normal network, the Price's model [25]. The latter was originally thought to describe the formation of citation networks, where each node represents a paper and a directed link, a citation from one paper to another one. The model exploits a preferential attachment principle where the total number of the nodes (n) is fixed and also the average out-degree for each node is fixed (m). At each step a new node is added and m links - on average - are created pointing from this node to existing nodes, following the principle that papers (nodes) will be cited

each step proportionally to their previous number of citations. Once the system contains n nodes the process stops and the resulting network is a regular DAG whose in-degree distribution follows a power-law with an exponent $2 < \gamma < 3$ [3]. An example of the pseudo-spectrum of such network is presented in Fig. 8 (left panel).

To make a link with existing models of networks generation we decided to start with three well studied topologies, Erdős-Rényi (ER) [22], Watts-Strogatz (WS) [23] and Barabási-Albert (BA) [24]. Let us observe that each model exists both in the unweighted than weighted versions, the role of the weights is to improve the non-normality of the binary case (see for instance Fig. 3 panel d).

The ER generalisation is straightforward, any possible couple of nodes is considered and with probability p_{ER} a link is set whose weight is drawn from a distribution $\mathcal{N}(0, \sigma)$ (or simply with unitary weight in the case of unweighted network).

In the panel (a) of the Fig. 3 in the main text, we report the ϵ -pseudo spectrum for several values of ϵ ; one can observe that the pseudo-spectrum resembles a “passion fruit”, black seeds represent the complex eigenvalues location while the coloured shells the ϵ -levels of the pseudo spectrum. Remark that the almost circular shape follows from the circular law. Moreover (bottom left panel) the non-normality increases as the distribution of the weights becomes broader, i.e. σ takes large values, and reaches the maximum when the adjacency matrix is a random one [40], i.e. $p_{ER} = 1$.

To build an unweighted non-normal Watts-Strogatz network we initially consider an undirected 1D ring where each node is connected to its $k/2$ (being k an even integer) neighbours on the left and on the right; then we iteratively check all the coupled of linked nodes, using any order, and with probability p_{WS} we rewired the directed link. The ϵ -pseudo spectrum reported in the panels (b) and (e) of the Fig. 3 in the main text shows that the network becomes more non-normal when the rewiring probability is higher, i.e. $p_{WS} \rightarrow 1$, and the connectivity of the initial regular (directed) graph is lower. This can be understood by observing that with $k = 2$ and $p_{WS} \sim 1$, many links are rewired and the probability to destroy the ring-like structure is very high, determining thus the presence of directed paths. If k is large, or p_{WS} is small, the initial ring-like structure will persist reducing the non-normality.

Following the same idea of the small-world topology in [13], we have extended the Newman-Watts algorithm to the case of non-normal networks. Here we started from a clockwise directed ring with weights chosen from a uniform distribution $\mathcal{U}[0, \gamma]$, then with a probability p_{NW} long-range directed links were added with uniform weights drawn from $\mathcal{U}[0, 1]$. To consider also some inertia in our model, we added some weak reciprocal links (whose weights are again drawn from $\mathcal{U}[0, 1]$) on the initial ring with probability p_R . The resulting model can thus exhibits different levels of non-normality tuning

the parameter γ [13].

Non-normal dynamics of networked non-linear systems

The intuitive meaning of the pseudo-spectrum

The pseudo-spectrum is an important and relatively recent mathematical tool which has already provided new important insights in different fields of science where non-normality emerges [17]. However, as we already anticipated in the main text, the non-normality has not yet been already observed and deeply studied in the framework of complex networked non-linear systems. While the linear behaviour is quite well understood, the bridge between pseudo-spectrum and non-linear dynamics is not completely set. Based on this fact, we here give a short description to explain the effect that the non-normality has on the stability of non-linear systems, $\dot{\mathbf{x}} = \mathbf{f}(\mathbf{x})$ where $\mathbf{f}: \mathbb{R}^n \rightarrow \mathbb{R}^m$ is a vectored-valued non-linear function.

The problem of the local linear stability is tackled by performing a Taylor expansion about a given fixed point \mathbf{x}^* , $\mathbf{f}(\mathbf{x}^*) = 0$. The evolution of the perturbation ϵ near the equilibrium \mathbf{x}^* is then given by:

$$\dot{\epsilon} = \left(\mathbf{Df}(\mathbf{x}^*) + \frac{1}{2!} \epsilon^T \mathbf{D}^2 \mathbf{f}(\mathbf{x}^*) \right) \epsilon + \dots, \quad (5)$$

where $\mathbf{Df}(\mathbf{x}^*)$ and $\mathbf{D}^2 \mathbf{f}(\mathbf{x}^*)$ are respectively the Jacobian matrix and the Hessian tensor of the non-linear function \mathbf{f} , both evaluated at the fixed point. Equation (5) has been purposely written to bring immediately to the fore the link with the pseudo-spectrum. In fact, the term $\frac{1}{2!} \epsilon^T \mathbf{D}^2 \mathbf{f}(\mathbf{x}^*)$ can be thought to be a matrix perturbation imposed to the Jacobian one, $\mathbf{Df}(\mathbf{x}^*)$.

The same problem of the local linear stability can be more rigorously analysed as following [45]. Let $\phi^t(\mathbf{x}_0)$ be the solution of the nonlinear ODE with initial datum $\mathbf{x}(0) = \mathbf{x}_0$, then one can define the matrix $\mathbf{L}(t) := \frac{\partial \phi^t(\mathbf{x}_0)}{\partial \mathbf{x}_0}$, describing the variation of the solution at some given time $t \geq 0$ as a function of the initial datum. One can then prove that \mathbf{L} is the unique solution of the matrixial system

$$\begin{cases} \dot{\mathbf{L}} = \frac{\partial \mathbf{f}(\mathbf{x})}{\partial \mathbf{x}}|_{\mathbf{x}=\phi^t(\mathbf{x}_0)} \mathbf{L} \\ \mathbf{L}(0) = \mathbf{1}. \end{cases}$$

Let us separate the linear part and the nonlinear one in $\mathbf{f}(\mathbf{x})$ by assuming the origin to be an equilibrium point and thus writing $\mathbf{f}(\mathbf{x}) = \mathbf{Ax} + \mathbf{g}(\mathbf{x})$, then the previous equation rewrites:

$$\begin{cases} \dot{\mathbf{L}} = \left(\mathbf{A} + \frac{\partial \mathbf{g}(\mathbf{x})}{\partial \mathbf{x}}|_{\mathbf{x}=\phi^t(\mathbf{x}_0)} \right) \mathbf{L} = (\mathbf{A} + \mathbf{G}(t)) \mathbf{L} \\ \mathbf{L}(0) = \mathbf{1}, \end{cases}$$

Because of its definition, the matrix $\mathbf{L}(t)$ can be used to describe the time evolution of any fixed vector \mathbf{v}_0 ; indeed let $\mathbf{v} = \mathbf{Lv}_0$, then

$$\dot{\mathbf{v}} = \dot{\mathbf{L}}\mathbf{v}_0 = (\mathbf{A} + \mathbf{G}(t)) \mathbf{Lv}_0 = (\mathbf{A} + \mathbf{G}(t)) \mathbf{v}.$$

Finally, assuming \mathbf{v}_0 to denote the departure from the equilibrium, then the last equation states that its time evolution is driven by the matrix $\mathbf{A} + \mathbf{G}(t)$, where the rightmost term can be considered as a perturbation of the linearised system $\dot{\mathbf{x}} = \mathbf{Ax}$.

The main point is that the perturbation depends on time in both cases and thus we are dealing with the stability question of a non-autonomous dynamical system. It is well known that in this framework, analytical solutions are available in very few cases, e.g. once periodic orbits do exist and one recurs to Floquet theory [46], however what matters for our purpose is to control the growth of the perturbation matrix, being directly related to the levels of the pseudo-spectrum. Let us observe that a similar analysis has been previously proposed in [17].

Generalised Lotka-Volterra model

The Generalised Lotka-Volterra (GLV) equations provide a perfect setting to model all kinds of trophic relationships that can arise between different species in a given ecosystem, indeed they can describe diverse interactions such as cooperation or competition (or a mix between them) depending on the choice of the community matrix. The set of equations governing the GLV are given by [9]:

$$\frac{dx_i}{dt} = x_i \left(r_i - s_i x_i + \sum_{j \neq i} M_{ij} x_j \right), \quad \forall i = 1, 2, \dots, N. \quad (6)$$

Here r_i are the intrinsic rates of birth if $r_i > 0$, meaning that species i can reproduce itself in absence of other species and in abundance of resources; or death ($r_i < 0$) in the sense that the population of species i will decline in absence of other species (e.g. preys). The constants s_i which should always be considered positive, represent the finite carrying capacity of the ecosystem (limited resources) and prevent the species i to grow indefinitely. An important role is played by the community matrix \mathbf{M} which entries M_{ij} (M_{ji}) represent the influence of species j on i (the influence of i on j). Observe that we assume $M_{ii} = 0, \forall i$, namely the community matrix describes only the inter-species interactions, while the intra-species interactions have been cast into s_i .

Usually the network described by the community matrix has been considered to be symmetric meaning that both species equally influence each others. However, experimental data (see Table I and SM) have shown that this is not generally true and that the community matrix can have strong asymmetric shape yielding to a strong non-normality. In order to model a competitive type of dynamics between the two species i and j we consider that both $M_{ij}, M_{ji} < 0$ and denote this case by $(-/-)$; in other words, this means that both species are mutually loosing from the presence of the other. In a similar way a prey-predator system is modelled by assuming $M_{ij} < 0, M_{ji} > 0$, hereby denoted by $(-/ +)$, where the

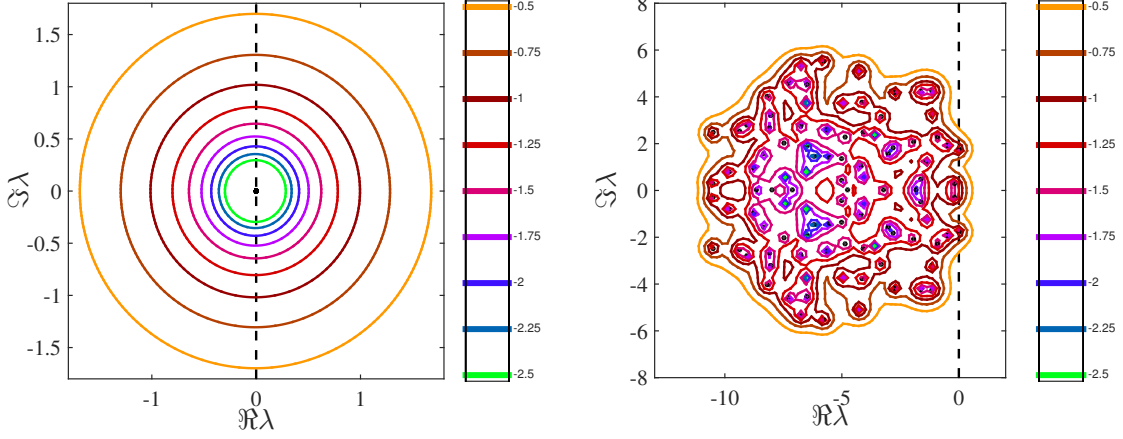


FIG. 8. **The spectra and pseudo-spectra of non-normal networks.** On the left panel we show the spectrum (black dot), consisting of a highly degenerate eigenvalue, and several ϵ -levels (coloured curves) of the pseudo-spectrum of the Price's network, with parameters $m = 3$ and $n = 100$ nodes. On the right panel we report the spectrum (black dots) and the pseudo-spectrum (coloured curves) of the non-normal Newman-Watts model with parameters $p_{NW} = 0.3$, $p_R = 0.1$, $\gamma = 1$ and $n = 100$ nodes. For the former network one can observe a quite large ϵ -pseudo abscissa while the same quantity is very small for the network on the right. The almost circular shape of the spectrum of this second case is reminiscent of the circular law. The pseudo-spectra have been numerically computed using the software *Eigtool* [34].

predator is gaining from the presence of the prey which on the other side is loosing because of the presence of the former. The last situation is when both species are getting profit of the presence of each other. In this case $M_{ij} > 0, M_{ji} > 0$, for short (+/+). This latter case is however less realistic because it implies that both species increases indefinitely because of the interactions. Let us finally observe that if an interaction exists such that the link $j \rightarrow$ has large positive (negative) weight, then we allow the reciprocal link to also exist, but to be small and negative (positive), in other words we are not considering the peculiar cases (0/+) and (0/−) sometimes described in the literature.

In the following we will adopt the method based on the

work of Chen and Cohen [47], as already done in the literature [8, 9]. More precisely, we hypothesise the existence of a positive equilibrium solution \mathbf{x}^* , that without loss of generality can be assumed to be of the form $x_i^* = 1$, for all i , after a suitable choice of the growth/death rates r_i .

At this point the Master Stability function of the GLV model depends solely on the spectrum (pseudo-spectrum) of the matrix $\mathbf{M} - \text{diag}(s)$, namely the community matrix from which we remove the matrix whose diagonal contains the inter-species strengths s_i . The problem is hence mapped to the framework proposed by May [7, 8] where the stability directly depends on species interactions.

-
- [41] G. H. Golub and C. F. van Loan, *Matrix Computations*, Johns Hopkins University Press 3ed (1996)
 - [42] M. G. Neubert, H. Caswell and J. D. Murray, *Math. Biosci.*, **175**, 1–11 (2002)
 - [43] We assume thus the definition of adjacency matrix such that $A_{ij} = 1$ if there is a link pointing from j toward i .
 - [44] P. J. M. van Laarhoven and E. H. L. Aarts, *Simulated*

- annealing*, Springer (1987)
- [45] V. I. Arnol'd, *Ordinary differential equations*, Springer (2006)
- [46] C. Chicone, *Ordinary differential equations with applications*, Springer-Verlag (1999)
- [47] X. Chen and J. E. Cohen, *J. Theor. Biol.*, **212**, 223–235 (2001)